Concentrated Mixed Cation Acetate "Water-in-Salt" Solutions as Green and Low Cost High Voltage Electrolytes for Aqueous Batteries

Journal:	*Energy & Environmental Science*
Manuscript ID	EE-ART-03-2018-000833.R1
Article Type:	Paper
Date Submitted by the Author:	27-Jun-2018
Complete List of Authors:	Lukatskaya, Maria R.; Stanford University, Chemical Engineering Feldblyum, Jeremy; Stanford University, Chemical Engineering Mackanic, David ; Stanford University, Chemical Engineering Lissel, Franziska; Leibniz Institute of Polymer Research Michels, Dominik; KAUST, Computational Sciences Group Cui, Yi; Stanford University, Department of Materials Science and Engineering Bao, Zhenan; Lucent Technologies, Bell Labs

Energy and Environmental Science

ARTICLE

Concentrated Mixed Cation Acetate "Water-in-Salt" Solutions as Green and Low Cost High Voltage Electrolytes for Aqueous Batteries

Received 00th January 20xx,
Accepted 00th January 20xx

DOI: 10.1039/x0xx00000x

www.rsc.org/

Maria R. Lukatskaya[1], Jeremy I. Feldblyum[1,2], David G. Mackanic[1], Franziska Lissel[3], Dominik L. Michels[4], Yi Cui[5], Zhenan Bao[1,*]

Electrolyte solutions are a key component of energy storage devices that significantly impact capacity, safety, and cost. Recent developments in "water-in-salt" (WIS) aqueous electrolyte research have enabled the demonstration of aqueous Li-ion batteries that operate with capacities and cyclabilities comparable with those of commercial non-aqueous Li-ion batteries. Critically, the use of aqueous electrolyte mitigates safety risks associated with non-aqueous electrolytes. However, the high cost and potential toxicity of imide-based WIS electrolytes limit their practical deployment. In this report, we disclose the efficacy of inexpensive, non-toxic mixed cation electrolyte systems for Li-ion batteries that otherwise provide the same benefits as current WIS electrolytes: extended electrochemical stability window and compatibility with traditional intercalation Li-ion battery electrode materials. We take advantage of the high solubility of potassium acetate to achieve the WIS condition in a eutectic mixture of lithium and potassium acetate; with water-to-cation ratio as low as 1.3. Our work suggests an important direction for the practical realization of safe, low-cost, and high-performance Li-ion batteries.

Introduction

Concerns of safety and cost are increasing as usage of batteries in various applications ranging from electronic devices and electrical vehicles to grid storage increases.[1-3] Although batteries containing organic electrolytes can demonstrate excellent energy densities, there are considerable safety concerns associated with their flammability and toxicity.[4, 5] Aqueous electrolytes can serve as a safer alternative, however, their use is limited due to energy density limitations stemming from the narrow electrochemical thermodynamic stability window of water of 1.23 V ($E = CV$, where E is the energy, C is capacity and V is the operation voltage window of the battery).[5, 6]

Recently, water-in-salt (WIS) electrolytes were proposed as a new approach to electrolytes that allows extending the voltage window of water-based electrolytes to ~3 V.[7] WIS electrolytes, a sub-class of solvent-in-salt electrolyte systems[8, 9], are defined as such in which dissolved salt outnumbers water by both volume and mass.[7] As electrolytes, WIS solutions benefit from the decreased activity of water molecules occurring when the solution salt concentration is high enough that no "free" water is present, i.e., all water molecules are a part of ion solvation shells. The WIS electrolyte concept was first demonstrated in batteries using 20 molal (20 m) aqueous solutions of lithium bis(trifluoromethanesulfonyl)imide, LiTFSI, for which the Li^+:H_2O molar ratio is 2.5.[7] Moreover, due to high salt concentration, increased anion interaction enabled formation of a solid electrolyte interface (SEI) layer as a result of the electrochemical decomposition of the $TFSI^-$ anion. The role of the SEI layer was emphasized as the dominant reason to achieve extended voltage window. Subsequent publications following this work allowed additional widening of the voltage window using organic imide hydrate melts of LiTFSI and lithium bis(pentafluoroethanesulfonyl)imide (LiBETI, $LiN(SO_2C_2F5)_2$) and enabled utilization of traditional battery electrode materials such as $Li_4Ti_5O_{12}$ as an anode and $LiNi_{0.5}Mn_{1.5}O_4$ as a cathode.[10]

Despite the remarkable improvement in the voltage window for current WIS systems, economic and environmental concerns that hinder real-world applications remain unresolved. In particular, the aforementioned LiTFSI salt has limited large-scale availability, whereas other hydrate melt components, such as LiBETI, are only available in limited quantities at a high price > 40 $/g.[11] Another

[1]Department of Chemical Engineering, Stanford, California, 94305, USA
[2]Department of Chemistry, University at Albany, SUNY, Albany, New York, 12222, USA
[3]Leibniz Institute of Polymer Research, 01069 Dresden, Germany
[4]Computational Sciences Group, KAUST, Thuwal, 23955, Kingdom of Saudi Arabia
[5]Department of Materials Science and Engineering Stanford University Stanford, California, 94305, USA
*Correspondence and requests for materials should be addressed to Zhenan Bao (zbao@stanford.edu)
† Electronic Supplementary Information (ESI) available: [details of any supplementary information available should be included here]. See DOI: 10.1039/x0xx00000x

concern is caused by limited amounts of lithium deposits in the Earth's crust, in comparison to deposits of sodium (Na) and potassium (K). Hence, the actual amount of lithium salt used to make the electrolyte is an important parameter to consider. For example, 1 L of LiTFSI-based WIS electrolyte would require ~5 times more lithium compared to traditional 1 m electrolytes. Moreover, there are substantial environmental concerns that involve the practical use of the noted above organic imide salts that are considered toxic to the environment. For instance, LITFSI possesses acute oral and dermal toxicity (Category 3), causes skin corrosion (Category 1B), and exhibits chronic aquatic toxicity (Category 3).[12] All these factors make practical implementation of the current WIS electrolyte chemistry into actual commercial energy storage devices challenging. On the other hand, the main challenge in selection of the new formulations of WIS electrolytes is caused by the lack of salts having water solubility high enough to satisfy the WIS condition and to provide an extended voltage window. Moreover, even fewer salts with lithium as a cation can satisfy this requirement due to the generally lower solubility of Li-based salts vs. salts based on other group A cations such as Na^+ and K^+.[13]

Herein we propose potassium acetate-based WIS electrolytes that can provide the same benefit of the extended voltage window as LiTFSI-based electrolytes and, once combined with lithium acetate, demonstrate compatibility with traditional Li-ion battery electrode materials but at the same time are low-cost and environmentally benign.

Results and discussion

Highly concentrated lithium-potassium acetate aqueous mixtures and their physicochemical properties

Concentrated potassium acetate, KCH_3COO, (KOAc) solutions satisfy the WIS condition by achieving molalities up to 27 m, corresponding to extremely small water amounts reaching 27.4 wt.%, or ~2 water molecules per potassium cation. To enable immediate compatibility with standard Li-ion intercalation anodes and cathodes, concurrent maximum solubility of lithium and potassium acetates in water was evaluated at different LiOAc to KOAc ratios (**Figure 1a**). The eutectic ratio was established to occur at a LiOAc molar fraction of 0.2, at which maximum solubility of salts is achieved with only ~1.3 water molecules per cation: 32 m KOAc – 8 m LiOAc ($Li_{0.2}K_{0.8}OAc \bullet 1.3H_2O$). For our further studies we focused on this eutectic composition and compared it to 27 m KOAc and dilute acetate solutions when needed.

Table 1 summarizes physicochemical properties of 27 m KOAc and the eutectic composition, 32 m KOAc – 8 m LiOAc. Interestingly, the observed density of the eutectic composition is smaller comparted to 27 m KOAc, which can be attributed to the less effective liquid "packing" due to the size differences of the K^+ and Li^+ cations. This also correlates well with molecular dynamics (MD) simulation results, which predicted densities of 1.47 (±0.05) g/cm^3 and 1.38 (±0.17) g/cm^3 for 27 m KOAc and 32 m KOAc – 8 m LiOAc, respectively (**Table 1** and **Figure 1 f** and **h**). Lithium-free solutions possess quite high viscosity (25 mPa/s) combined with conductivity of 31.4 mS/cm at 25 °C. Whereas the eutectic composition (32 m KOAc – 8 m LiOAc) is characterized by a viscosity of 374 mPa/s and a conductivity of 5.3 mS/cm at 25 °C, this value for conductivity is comparable to the few mS/cm observed for standard lithium ion non-aqueous electrolytes[14, 15] and other previously reported WIS formulations[7, 10]. Walden plot analysis demonstrates "good ionic" behavior of the superconcentrated acetate solutions (**Figure S1**).

In order to further examine interactions in these highly concentrated solutions, calorimetric analysis (**Figure 1b**) in conjunction with nuclear magnetic resonance (NMR) studies (Figure 1c and d) and molecular dynamics (MD) simulations (**Figure 1 e-h**) were performed and compared with the behavior of the respective 1 m KOAc and LiOAc solutions.

To characterize the thermal properties of the eutectic and associated solutions, differential scanning calorimetry (DSC) was performed. **Figures 1b** and **S2** show the differential scanning thermograms of 1 m LiOAc, 1 m KOAc, 27 m KOAc, 27 m KOAc – 6 m LiOAc, and 32 m KOAc – 8 m LiOAc aqueous solutions. Both 1 m solutions exhibit properties expected for aqueous solutions of moderate salt concentrations: clear melting transitions occur at -3.5 °C and -3.1 °C for the 1 m KOAc and LiOAc solutions, respectively, close to the expected value (-3.7 °C) for a 1 m salt solution with a completely dissociated salt[16] and lower than that of pure water (0 °C). In contrast, the saturated salt solutions do not show the expected peaks corresponding to melting transitions over the entire range examined. The 27 m KOAc solution exhibits a gentle slope in the heat flow, suggesting that sluggish kinetics may obscure clear evidence of a phase transition by DSC analysis. A similar change in heat flow occurs for the eutectic solution. To clarify the temperature at which these solutions melt, both were observed by visual inspection to solidify by immersion a -78 °C cooling bath. Both solutions were then warmed, and by the time they reached -40 °C, they were observed to have melted. Compared to their dilute counterparts, the heat capacities of the saturated LiOAc and eutectic solutions dropped dramatically. While the heat capacities of the 1 m solutions of LiOAc and KOAc at 25 °C were calculated

Table 1**. Physicochemical properties of the solutions at 25 °C**

Solution	Salt molar fraction (%)	Density experimental/ from MD (g/cm^3)	Viscosity (mPa/s)	Conductivity (mS/cm)
27 m KOAc	32.7	1.45 / 1.47(±0.05)	32	31.4
32 m KOAc – 8 m LiOAc	41.9	1.33 / 1.38 (±0.17)	374	5.3

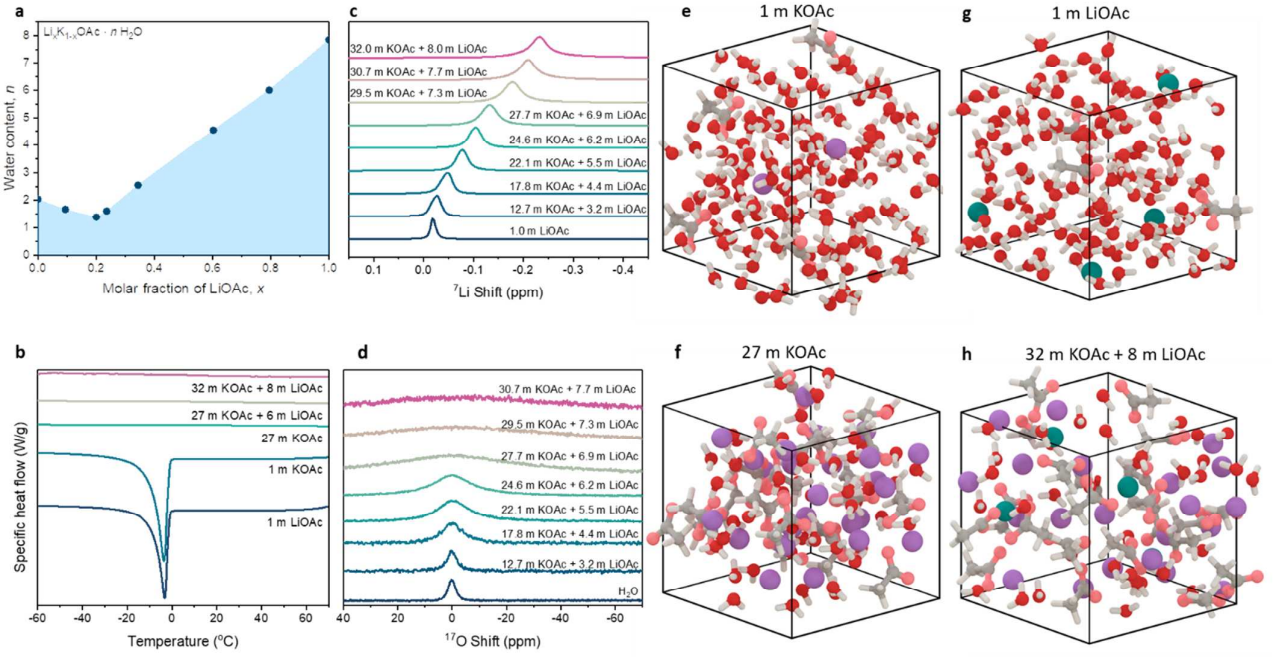

Figure 1. **Physicochemical properties of the lithium and potassium acetate solutions in water**. **a**, Measured liquidus line of the $Li_xK_{1-x}OAc$ salt-water mixtures. **b**, Vertically offset differential scanning calorimetry data of solutions collected at a rate of 1 °C/min. **c**, ^{7}Li NMR spectra. **d**, ^{17}O NMR spectra. Data are vertically offset and normalized for ease of visualization. **e-h**, Visualization of the equilibrated electrolyte systems after 4 ns: **e**, 1 m KOAc, **g**, 1 m LiOAc, **f**, 27 m KOAc, **h**, 32 m KOAc − 8 m LiOAc. Color scheme: violet: K, green: Li, red: O, grey: C, white: H.

from the DSC data to be 3.6 and 3.5 J g^{-1} K^{-1}, respectively, the heat capacities at 25 °C of the saturated KOAc and eutectic solutions were 2.4 and 2.0 J g^{-1} K^{-1}, respectively. These low heat capacities attest to the significant reduction in mobility and hydrogen bonding between water molecules in solution.

A dilution series were performed in conjunction with ^{7}Li NMR spectroscopy to probe the coordination environment of Li^+ in the WIS electrolytes. **Figure 1c** shows that increasing salt concentration in the dual-salt electrolytes results in an upfield shift in the ^{7}Li NMR spectrum. An upfield shift is indicative of ion shielding, or increased Lewis basicity in the vicinity of the lithium cation.[17]

Approaching the limit of high concentration, the solvation shell of the different ions strongly interpenetrate, and the primary coordination sphere of the Li^+ contains not only water molecules but also anions. The presence of anions in the coordination sphere of Li^+ leads to increased electron density on the cation, resulting in the observed upfield peak shift. The linewidths of the ^{7}Li NMR spectrum are relatively narrow for all of the electrolytes investigated. The narrow linewidths are indicative of a fast exchange between the lithium cation and molecules in the solvation shell.[18] For the high concentration electrolytes, the line width increases marginally, again indicating complexation and pronounced interaction with the anions in solution. The results of MD simulations are consistent with the experimental observations: After reaching equilibrium, the respective ions in both 1 m solutions are fully separated by more than 5 Å with no interpenetration of the ionic hydration shells and the bulk of water molecules present outside the cationic hydration shells (fraction of free water ≥ 0.9), consistent with a salt-in-water system (**Figure S5 a** and **b**). For the highly concentrated 27 m KOAc and 32 m KOAc – 8 m LiOAc systems, the ionic hydration shells show a high degree of interpenetration with every water molecule present in at least one hydration shell at any given time (fraction of free water = 0). Also, the systems are characterized by a markedly high degree of interpenetration of the hydration shells and ion pairing with the fraction of ions fully shielded by water molecules is approximating 0 (**Figure S5 c and d**). Based on the MD simulations, the mixtures can consequently be described as a near-ideal WIS systems (**Figure 1 g** and **h**).

^{17}O NMR experiments were also performed to better understand the behavior of water in these water-in-salt systems. For KOAc, at concentrations nearing saturation, the characteristic water peak both shifts and broadens (**Figures S3, S4a, and S4b**). The same effect is observed in the mixed salt system (**Figures 1d, S3c, and S3d**). Peak broadening (**Figure S3c**) can be attributed to decreasing T_2 relaxation time, which in turn comes from the dramatically increased solution viscosity (*vide supra)*.[19, 20] Broadening is significantly more pronounced in the mixed salt system at the highest concentrations, as the achievable total salt molality is ~1.5 times higher compared with that of the 27 m KOAc solution. Especially above a molal concentration of 0.8 relative to the eutectic (C/C_0 > 0.8, where C is the total molality of the mixed salt

solution and C_0 is the molality of the eutectic WIS solution), considerable broadening occurs in the mixed salt system, with the FWHM increasing by a factor of up to 30 (**Figure S3c**). At these high concentrations, there are more than 0.6 cations (and an additional 0.6 anions) per water molecule. According to the MD simulations (*vide supra*), on average every water molecule interacts with more than one cation (counting only interactions in the first hydration shell).

For both the KOAc and the $Li_{0.2}K_{0.8}OAc$ solutions, the water peak shifts upfield (towards negative values) with increasing salt concentration. A dramatic shift to more negative values above concentrations of 0.8 relative to the eutectic suggests a pseudo phase transition of the state of water in the solution (**Figure S4c**, also supported by the dramatic increase in peak FWHM, **Figure 1d**). A shift to more negative values is indicative of the breaking of hydrogen bonds between water molecules[21], which is consistent with the strong interpenetration of solvation shells and presence of each water molecule in more than one ionic coordination sphere. The sharp change in both peak position and FWHM could be explained by the beginning of interpenetration of hydration shells at concentrations above 0.8 relative to the eutectic. Interpenetration of hydration shells exposes individual water molecules to significantly more charge per ion due to a reduction in average coordination number of individual ions. Such interpenetration of hydration shells is consistent with our findings from MD (*vide supra*) that in the first hydration shell, each water molecule interacts with an average of 1.3 cations in the mixed salt solution.

Electrochemistry in highly concentrated acetate electrolytes

The electrochemical stability window of 27 m KOAc and 32 m KOAc – 8 m LiOAc electrolyte solutions in combination with different current collector materials was evaluated using cyclic voltammetry (CV) at low scan rates of 0.2 mV/s and compared with the CV data obtained in 1 m KOAc electrolyte (**Figure 2 a-b**).

First, platinum (Pt) current collector was used to probe hydrogen evolution onset in highly concentrated acetate electrolytes: Pt was selected to ensure minimal kinetic limitations as it is known for its catalytic activity towards hydrogen evolution reaction[22, 23]. As can be seen from **Figure 2a**, a ~1.15 V extension of electrochemical stability window upon increase in KOAc salt concentration from 1 m to 27 m. An increased salt molality in 32 m KOAc – 8m LiOAc solution didn't result in additional voltage window extension and CV trace for it nearly coincides with 27 m KOAc. This can be explained by similar "state" of water molecules in both solutions, where each solvent molecule is a part of at least one ion solvation shell (**Figure 1**).

Next, stability window of electrolytes was probed using titanium (Ti) and glassy carbon electrodes as current collectors. Both current collector materials are characterized by large overpotentials for electrochemical water splitting and hence hydrogen and oxygen evolution reactions are expected to be suppressed over much extended potential range compared to Pt.[24] Indeed, further

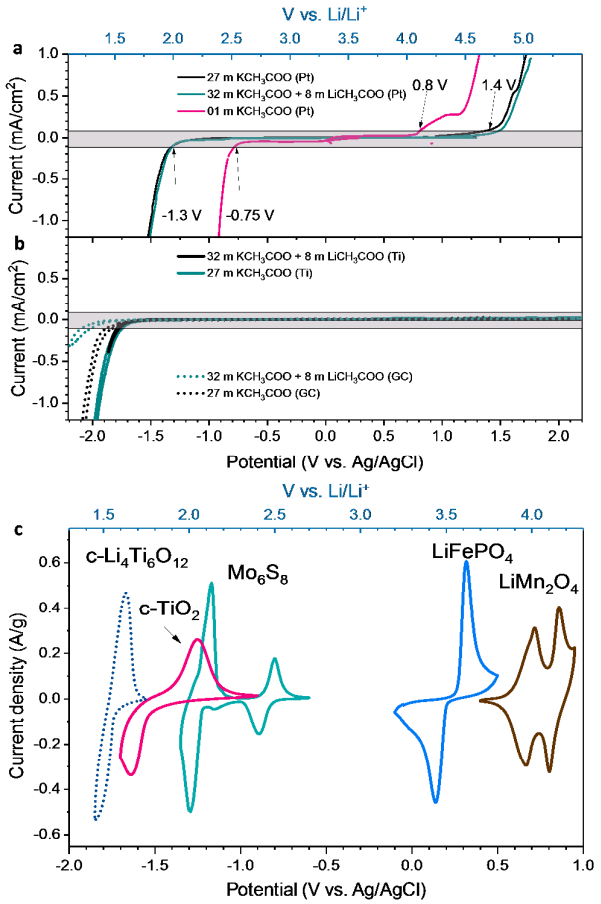

Figure 2. Cyclic voltammetry profiles collected at 0.2 mV/s for the acetate solutions using **a**, Pt foil and **b**, Ti foil and glassy carbon as current collectors. Shaded grey area represent current densities below 0.1 mA/cm^2, after which contribution of the water-splitting from current collectors is non-negligible. **c**, Cyclic voltammetry profiles collected in 32 m KOAc – 8 m LiOAc at 0.2 mV/s for c-TiO_2 (pink), Mo_6S_8(teal), $LiFePO_4$ (blue), $LiMn_2O_4$ (brown) with Ti current collectors and c-$Li_4Ti_5O_{12}$ on glassy carbon current collector.

increased stability window was observed for concentrated acetate solutions (**Figure 2b**). Almost identical profiles were observed in 27 m KOAc and 32 m KOAc – 8m LiOAc when Ti current collector was used (solid lines in **Figure 2b**). Whereas, the most pronounced extension in negative potential range was observed in 32 m KOAc – 8m LiOAc with glassy carbon current collector. The positive potential range of CV profiles are characterized by absence of any pronounced electrochemical features which can be explained by the surface passivation of current collector caused by anodic oxidation.[25]

As discussed above, presence of the Li^+ is essential to ensure compatibility with already developed electrode materials for Li-ion batteries. Therefore, to evaluate whether a mixed cation strategy would allow us to use already-developed Li-ion electrode systems, we performed CV characterization of the various typical anode and cathode materials in the 32 m KOAc – 8m LiOAc electrolyte. All tested materials demonstrated a set of reversible Li-ion

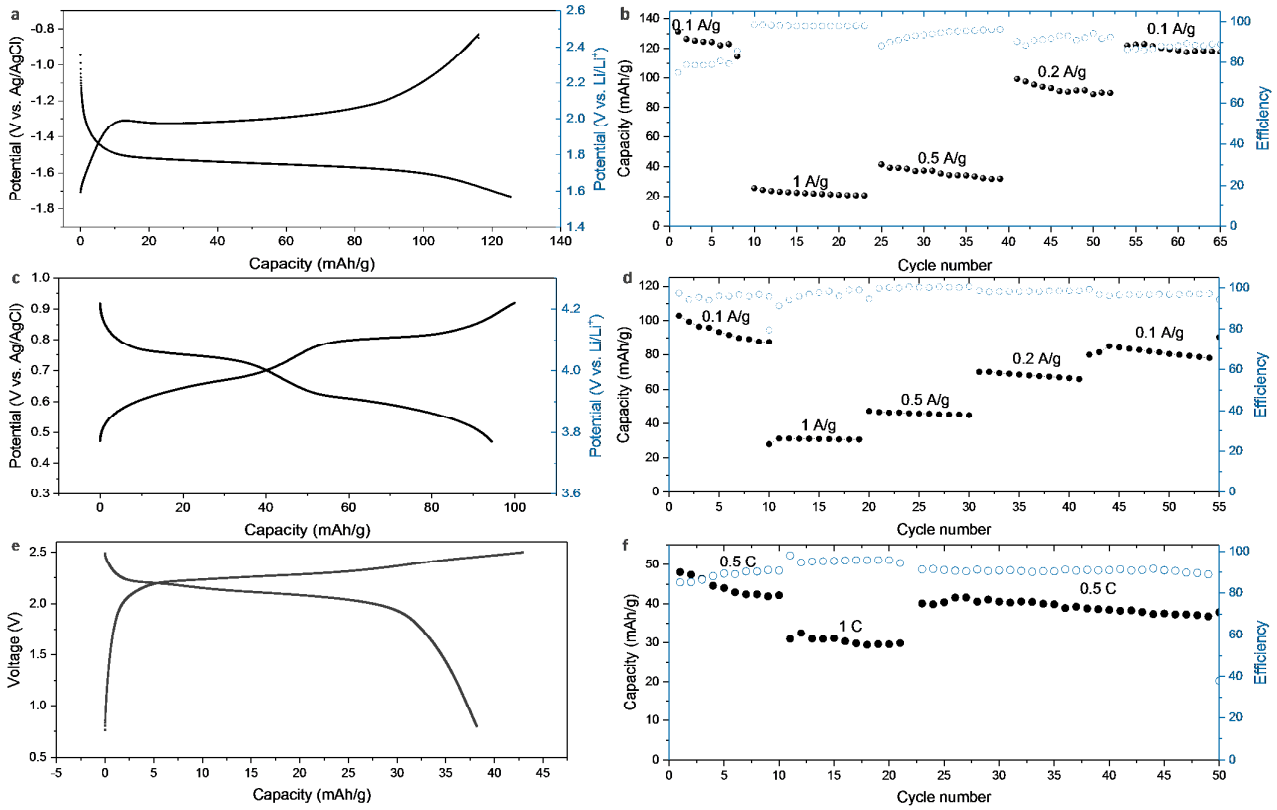

Figure 3. **Electrochemical performance of c-TiO_2 anode and $LiMn_2O_4$ cathode in 32 m KOAc – 8 m LiOAc**. Galvanostatic charge-discharge profiles for **a**, c-TiO_2 and **c**, $LiMn_2O_4$ and **e**, c-TiO_2/$LiMn_2O_4$ full cell collected at 0.5 C charging rate. Corresponding rate capability, capacity retention data and coulombic efficiency for **b**, c-TiO_2, **d**, $LiMn_2O_4$ and **f**, c-TiO_2/$LiMn_2O_4$ full cell.

intercalation peaks (**Figure 2c**). For anode materials, we first evaluated Mo_6S_8 (Chevrel phase), which was used for initial demonstration of the WIS concept by Suo et al.[7] The CV profile revealed a reversible second intercalation peak which is not attainable in standard dilute aqueous electrolytes due to much earlier onset of the electrochemical electrolyte decomposition[7] and a capacitance of 140 mAh/g when cycled galvanostatically at ~0.5 C rate **(Figure S6 a)**. Since in the past Mo_6S_8 was demonstrated to reversibly[26] intercalate larger cations such as Mg^{2+} we checked whether K^+ itself could participate in charge storage. To do so, the performance in 27m KOAc was tested (**Figure S6 b**). No electrochemical features related to intercalation were observed, which can be can be explained by the larger cation size of K^+ compared to Mg^{2+}.[27] From the comparison of the CV profiles with and without LiOAc it can be seen that the response can be clearly attributed to the reversible Li^+ intercalation and not K^+ and indicates the efficiency and importance of the mixed cation strategy.

Since CVs in 32m KOAc – 8m LiOAc with Ti and glassy carbon (GC) current collectors (**Figure 2b**) demonstrated extended voltage windows with negligible parasitic currents up to ~-1.8 V vs Ag/AgCl (1.5 V vs. Li/Li^+) and -1.95 V vs Ag/AgCl (1.35 V vs. Li/Li^+), we evaluated the performance of anodes with even lower intercalation potentials, such as TiO_2 and $Li_4Ti_5O_{12}$. Titanates are known to catalyze hydrogen evolution[28] and to suppress parasitic reactions and also improve conductivity, carbon-coated samples, respectively labelled as c-TiO_2 and c-$Li_4Ti_5O_{12}$, were prepared[29]. The resulting CV profiles revealed reversible Li^+ intercalation in both electrodes, however for c-$Li_4Ti_5O_{12}$ good performance was achieved when glassy carbon was used as a current collector whereas use of Ti resulted in noticeable concurrent parasitic process of electrolyte decomposition. This correlates well with the CVs of the bare current collectors (**Figure 2b**). In contrast, good performance was achieved with more practical Ti current collector for c-TiO_2, therefore we selected c-TiO_2 for further studies of the cycling stability by galvanostatic cycling at 0.1 A/g (~0.5 C rate) (**Figures 3a, S7a)**. c-TiO_2 electrodes demonstrated respectable cycling stability in 32m KOAc – 8m LiOAc electrolyte and maintained ~90 % of their original capacity after 55 cycles.

Suitable cathode materials were also evaluated. $LiFePO_4$ demonstrated reversible redox behavior with our WIS electrolyte (**Figure 2c**). However, to truly benefit from the extended voltage window of our electrolyte, we tested $LiMn_2O_4$ which offers higher intercalation potential. CV profiles of $LiMn_2O_4$ are identical to those one would expect in organic electrolytes, with well-resolved intercalation/deintercalation peak (**Figure 2c**). Electrodes also demonstrated stable cycling performance with 90% of capacitance

retained after 100 cycles (**Figure S7b**). We surmise that the cycling stability of anode and cathode materials can be improved further by introduction of small amounts of additives to the present electrolyte formulations in the same manner as is commonly done with conventional organic[14] and aqueous battery systems[30, 31].

In addition, we evaluated the rate performance of both c-TiO_2 (**Figure 3b**) and $LiMn_2O_4$ (**Figure 3d**) in 32m KOAc – 8m LiOAc and compared it with the rate performance of the same electrodes in standard organic electrolyte, 1M $LiPF_6$ in EC-DEC (**Figures S8a and b**). Despite the higher solution viscosity, a comparable ($LiMn_2O_4$) or superior (c-TiO_2) rate performance was observed when 32m KOAc – 8m LiOAc is used as electrolyte instead of 1m $LiPF_6$ in EC-DEC.

Finally, the performance of a c-TiO_2/ $LiMn_2O_4$ full cell was evaluated. The cell delivered an operation voltage window of 2.5 V (**Figure 3e**). Galvanostatic cycling revealed stable cycling performance of the cell with capacities of ~45 mAh/g (**Figure 3f**), which is comparable with those previously reported for organic imide-based WIS systems.[7, 29]

Conclusions

In summary, we demonstrate the use of a highly concentrated lithium-potassium acetate mixture in water, enabling us to push the water-to-salt ratio to the lowest amount yet reported for a battery WIS electrolyte, reaching a water-to-cation molar ratio of 1.3. Molecular dynamics simulations confirmed the true WIS nature of this system, where there is no free water present and cation solvation shells are comprised solely of shared water molecules with anions present as ligands in the cationic coordination sphere. This correlates well with ^{7}Li and ^{17}O NMR data which clearly indicate disruption of water-water hydrogen bonds and strong ionic interactions. Our WIS electrolytes exhibit conductivities comparable to or higher than typical organic electrolytes and an electrochemical stability window of 3V for highly concentrated potassium and lithium-potassium acetate mixtures.

Typical non-aqueous Li-ion battery materials such as $Li_4Ti_5O_{12}$, TiO_2 and $LiMn_2O_4$ show reversible Li-ion intercalation with good cycling stability using the our WIS electrolyte. Mixed cation acetate electrolytes are cheap and environmentally friendly. Moreover, we show that amount of lithium in the mixtures can be varied over a wide range allowing for future further minimization of the lithium salt being used in the mixture. We believe that presented here bi-cation approach can be extended to other salt systems as well and move water-based batteries closer to consumer electronics and grid energy storage.

Methods

Water-in-salt solutions preparation. Potassium acetate (anhydrous, ≥99.0%) and lithium acetate (anhydrous, 99.95%) were purchased from Sigma Aldrich and thoroughly dried under vacuum and transferred to N_2-filled glovebox. Then, in glovebox, calculated amounts of salts were placed in 20 ml glass vials and sealed under N_2 using crimp caps with septa. Calculated volume of deionized MilliQ water was then added at ambient atmosphere using syringe. Lastly, solutions were left overnight for complete salt dissolution.

Preparation of carbon-coated TiO_2 and $Li_4Ti_5O_{12}$ anode powders. Nano-sized anatase TiO_2 was purchased from Sigma-Aldrich and $Li_4Ti_5O_{12}$ was purchased from MTI Corporation. Carbon-coated samples of TiO_2 and $Li_4Ti_5O_{12}$ (abbreviated accordingly as c- TiO_2 and c-$Li_4Ti_5O_{12}$) were prepared using carbothermal reduction of sucrose in TiO_2 (or $Li_4Ti_5O_{12}$): sucrose mixture with mass ratio of 2:1 at 600^{o}C for 2 hours in N_2 atmosphere.

Cathode materials. $LiMn_2O_4$ was purchased from Sigma Aldrich and $LiFePO_4$ was purchased from MTI Corporation.

Electrode preparation. For all active materials the same procedure was followed to generate free-standing composite electrodes. First, active material powder, polytetrafluoroethylene (PTFE) binder solution (60 wt.% in H_2O, Aldrich), and carbon black powder were mixed together with ethanol (200 proof, Sigma Aldrich) until a homogenous slurry was formed. Then, once the ethanol evaporated at R.T., the dried slurry was transferred onto a glass surface, and a few ethanol drops were added and subjected to mechanical processing: repeated kneading with a stainless-steel spatula until powder particles started sticking together before finally rolling into a free-standing film. The resulting electrodes – were used for all electrochemical experiments – had mass density per unit area of ~3 mg/cm^2 containing 85 wt. % of active material, 5 wt. % of PTFE, 10 wt. % of carbon black.

Activated carbon (AC) counter electrodes. Activated carbon film electrodes were prepared following the same procedure as above but without any conductive additive. The resulting electrode composition was 95 wt. % of YEC-200 activated carbon (Yihuan Carbon Co., Ltd, China) and 5 wt. % of the PTFE. Electrodes had mass density per unit area of 10-25 mg cm^{-2}.

Liquidus line measurements. To measure the liquidus line of the of the $Li_xK_{1-x}OAc$ salt-water mixtures (Figure 1a), LiOAc and KOAc were mixed at varying mole fractions in a N_2-filled glovebox. The solid mixtures were transferred into septum-sealed vials, which were removed from the glovebox. To each vial, water was added incrementally via volumetric glass syringe, and after each addition of water, the vials were sonicated for ~1 hour at ~35 °C. Water was added after each heating/sonication step until the salt mixture was completely dissolved *after cooling to room temperature*. Vials were left at room temperature (~22 °C) for a minimum of 3 days to ensure the salt remained dissolved.

Solution conductivity measurements. Solutions conductivity was measured using Oakton™ CON 6^{+} conductivity meter at 25 ◦C. Prior each measurement, accuracy of was ensured by calibration in 12880 µS/cm calibration solution (HI7030L by Hanna Instruments).

Density measurements. Density of the solutions was measured using "density" mode with MX5 Microbalance (Mettler Toledo). Each measurement was repeated at least 5 times.

Electrochemical measurements and set-up. All electrochemical tests (cyclic voltammetry, galvanostatic cycling) were performed

using either MPG-2 or VPS potentiostats (Biologic) in custom-modified three-electrode PFA Swagelok cells. The reference electrodes were either Ag/AgCl in 1 M KCl (CH Instruments) or leakless Ag/AgCl in 3.4 M KCl (eDAQ). For most tests an overcapacitive activated carbon was used as a counter electrode, where counter electrode weight was at least 10 times more than weight of the working electrode. Platinum, glassy carbon and titanium current collectors used in this study were polished to the mirror finish using fine alumina powders and cleaned by consequent sonication in DI water and ethanol prior each use. The full cell was constructed with excess of $LiMn_2O_4$ (to compensate for the irreversible lithium consumption[29]). The mass ratio of 1:2 was used for c-TiO_2 to $LiMn_2O_4$. Galvanostatic cycling current densities for the full cell were calculated with regards to the TiO_2 weight.

^{7}Li Nuclear Magnetic Resonance (NMR). NMR spectra were obtained on a Varian Inova 300MHz NMR spectrometer. 5 mm glass NMR tubes (Cambridge Isotope Laboratories) were charged with 700 µL of the appropriate water-in-salt solution in air. NMR tubes were immediately sealed with plastic septa wrapped with parafilm to limit exposure to atmospheric moisture. ^{7}Li shifts were referenced to a 1.0 m sample of LiCl in deuterated water. Data was acquired without a deuterium lock, and the reference standard was measured before and after data collection to determine that no field drift occurred. Samples were analysed at 25 ± 0.1 °C. Data were processed in MestReNova 11.0.2.

^{17}O Nuclear Magnetic Resonance (NMR). NMR spectra were obtained on a Varian Inova 300. 5 mm glass NMR tubes (Cambridge Isotope Laboratories) were charged with 700 µL of the appropriate water-in-salt solution in air, followed by addition of 30 µL 10% ^{17}O-enriched H_2O (Cambridge Isotope Laboratories). NMR tubes were immediately sealed with plastic septa wrapped with parafilm to limit exposure to atmospheric moisture. Sample dilution was achieved by addition of H_2O (natural isotopic abundance) directly to the appropriate NMR tube, which was immediately resealed as described above. Samples were analysed at 25 ± 0.1 °C. Data were processed in MestReNova 11.0.2 for background and phase correction, and referencing the chemical shift of pure H_2O to 0 ppm.

Differential Scanning Calorimetry (DSC). DSC traces were obtained on a Q2000 (TA Instruments). Samples (~5 mg) were added to aluminum Tzero pans (TA Instruments) and hermetically sealed with a Tzero Sample Press (TA Instruments). Samples were first exposed to one heating/cooling cycle from -80 °C to 80 °C to -80 °C at a rate of 10 °C/min. Data were then obtained from -80 °C to 80 °C at a rate of 1 °C/min. Data were processed in TA Universal Analysis (TA Instruments).

Viscosity measurements. Viscosity measurements were obtained using an oscillatory rheometer (ARES-G2, TA Instruments). 30 mL water-in-salt solution was added to a sample cup, and the sample analysed in a cone and cup geometry.

Molecular dynamics (MD) simulations. Molecular dynamics (MD) simulations were performed for four different electrolyte systems, (A) 1 m KOAc, (B) 1 m LiOAc, (C) 27 m KOAc, (D) 32 m KOAc – 8 m LiOAc, in order to examine the composition of the hydration shell of both cations. Relevant data for the systems can be found in **Table S1**. For each system, the molecules were distributed randomly and the salts indiscriminately placed as independent ions to reflect the solubilized state to allow to disregard the hydration enthalpies and reduce the calculation time. Equilibrium runs for temperature T and pressure p were performed before an isothermal–isobaric (NPT) ensemble was set up and a Nose-Hoover thermostat and a barostat were used to control temperature and pressure.

An in-house developed molecular dynamic program was utilized for the simulations and an atom-centred isotropic dipole polarizability employed to represent Coulomb and polarization interactions, while the water-water repulsion-dispersion interactions were described using a Lennard-Jones potential and all other repulsion-dispersion interactions with a Buckingham potential. The Ewald summation method was used for all electrostatic interactions. Multiple time step integration was employed and the reciprocal part of Ewald updated at the largest of the multiple time steps. To get further efficiency, a semi-analytical integration was employed.[32]

Initial velocities for the MD production run were obtained according to the Maxwell-Boltzmann distribution with T = 296.15 K and p = 1 atm. For each system, the relative energy remains constant over the length of the production run with a maximum deviation of less than 4% with regards to the initial energy (see **Figure S9**). Please note that the oscillations are not increasing over time which is an additional indicator for the stability of simulation.

After a simulation time of around 3 ns, the systems reach a compositional equilibrium marked by a structurally steady state in which – excluding minor fluctuations – the average composition of the electrolyte is constant (see **Figure S5, A-D**). Continuing the simulation for up to 4 ns does not change the steady state.

The visualization of the molecular structures (see Figure 1) was realized utilizing the non-commercial Visual Molecular Dynamics VMD software.[33]

Conflicts of interest

There are no conflicts to declare.

Acknowledgements

We thank N. Shpigel and M.D. Levi at Bar-Ilan University for providing Mo_6S_8 and fruitful discussions and A.R. Akbashev at Stanford University for performing TEM characterization of the samples. This work was partially supported by the Assistant Secretary for Energy Efficiency and Renewable Energy, Office of Vehicle Technologies of the U.S. Department of Energy, under the Battery Materials Research (BMR) program. Part of this work was performed at the Stanford Nano Shared Facilities (SNSF), supported by the National Science Foundation under award ECCS-1542152. D.G.M. acknowledges support by the National Science Foundation Graduate Research Fellowship Program under Grant No. (DGE-114747). F.L. and D.L.M. gratefully acknowledge support from KAUST baseline funding and KAUST's Shaheen XC40 HPC infrastructure.

Notes and references

1. 1. D. H. Doughty and E. P. Roth, *The Electrochemical Society Interface*, 2012, **21**, 37-44.
2. D. Larcher and J. M. Tarascon, 2014, **7**, 19.
3. B. Dunn, H. Kamath and J.-M. Tarascon, *Science*, 2011, **334**, 928-935.
4. C. P. Grey and J. M. Tarascon, *Nat Mater*, 2017, **16**, 45-56.
5. L. Xia, L. Yu, D. Hu and G. Z. Chen, *Materials Chemistry Frontiers*, 2017, **1**, 584-618.
6. M. R. Lukatskaya, B. Dunn and Y. Gogotsi, *Nature Communications*, 2016, **7**, 12647.
7. L. Suo, O. Borodin, T. Gao, M. Olguin, J. Ho, X. Fan, C. Luo, C. Wang and K. Xu, *Science*, 2015, **350**, 938.
8. L. Suo, Y.-S. Hu, H. Li, M. Armand and L. Chen, *Nature Communications*, 2013, **4**, 1481.
9. Y. Yamada and A. Yamada, *Journal of The Electrochemical Society*, 2015, **162**, A2406-A2423.
10. Y. Yamada, K. Usui, K. Sodeyama, S. Ko, Y. Tateyama and A. Yamada, *Nature Energy*, 2016, **1**, 16129.
11. *Journal*.
12. Bis(trifluoromethane)sulfonimide lithium salt, MSDS No. 544094 [Online], Aldrich: Saint Louis, MO, http://www.sigmaaldrich.com/MSDS/MSDS/DisplayMSDSPage.do?country=US&language=en&productNumber=449504&brand=ALDRICH&PageToGoToURL=http%3A%2F%2Fwww.sigmaaldrich.com%2Fcatalog%2Fproduct%2Faldrich%2F449504%3Flang%3Den).
13. W. M. Haynes, in *CRC handbook of chemistry and physics*, CRC press, 91th edn., 2014, pp. 8-112.
14. K. Xu, *Chemical Reviews*, 2014, **114**, 11503-11618.
15. M. Ue and S. Mori, *Journal of The Electrochemical Society*, 1995, **142**, 2577-2581.
16. D. A. McQuarrie, P. A. Rock and E. B. Gallogly, *General chemistry*, WH Freeman, 1984.
17. M. C. Masiker, C. L. Mayne, B. J. Boone, A. M. Orendt and E. M. Eyring, *Magnetic Resonance in Chemistry*, 2010, **48**, 94-100.
18. S. H. Chung, K. R. Jeffrey and J. R. Stevens, *The Journal of Chemical Physics*, 1991, **94**, 1803-1811.
19. R. S. Macomber, *A complete introduction to modern NMR spectroscopy*, Wiley, 1997.
20. N. Bloembergen, E. M. Purcell and R. V. Pound, *Physical Review*, 1948, **73**, 679-712.
21. V. Maemets and I. Koppel, *Journal of the Chemical Society, Faraday Transactions*, 1997, **93**, 1539-1542.
22. S. Trasatti, *Journal of Electroanalytical Chemistry and Interfacial Electrochemistry*, 1972, **39**, 163-184.
23. I. Roger, M. A. Shipman and M. D. Symes, *Nature Reviews Chemistry*, 2017, **1**, 0003.
24. J. D. Benck, B. A. Pinaud, Y. Gorlin and T. F. Jaramillo, *PLOS ONE*, 2014, **9**, e107942.
25. G. Bewer, H. Debrodt and H. Herbst, *JOM*, 1982, **34**, 37-41.
26. D. Aurbach, Z. Lu, A. Schechter, Y. Gofer, H. Gizbar, R. Turgeman, Y. Cohen, M. Moshkovich and E. Levi, *Nature*, 2000, **407**, 724-727.
27. Y. Marcus, *Chemical Reviews*, 1988, **88**, 1475-1498.
28. M. Ni, M. K. H. Leung, D. Y. C. Leung and K. Sumathy, *Renewable and Sustainable Energy Reviews*, 2007, **11**, 401-425.
29. L. Suo, O. Borodin, W. Sun, X. Fan, C. Yang, F. Wang, T. Gao, Z. Ma, M. Schroeder, A. von Cresce, S. M. Russell, M. Armand, A. Angell, K. Xu and C. Wang, *Angewandte Chemie International Edition*, 2016, **55**, 7136-7141.
30. F. Wang, Y. Lin, L. Suo, X. Fan, T. Gao, C. Yang, F. Han, Y. Qi, K. Xu and C. Wang, *Energy & Environmental Science*, 2016, **9**, 3666-3673.
31. H. Kim, J. Hong, K.-Y. Park, H. Kim, S.-W. Kim and K. Kang, *Chemical Reviews*, 2014, **114**, 11788-11827.
32. D. L. Michels and M. Desbrun, *J. Comput. Phys.*, 2015, **303**, 336-354.
33. W. Humphrey, A. Dalke and K. Schulten, *Journal of Molecular Graphics*, 1996, **14**, 33-38.

Broader Context

Electrolytes are an essential component of energy storage devices. Electrolyte composition has a significant impact on the safety, price and performance of the battery. Intrinsically nonflammable aqueous electrolytes can offer safer battery operation and decreased associated toxicity, but suffer from a smaller electrochemical stability window (and hence energy density) compared to traditional organic electrolytes. Recently proposed highly concentrated “water-in-salt” electrolytes offer extended electrochemical stability window. However, due to a lack of lithium salts having water solubility high enough to satisfy the water-in-salt condition, the selection was limited to toxic and high cost organic imides. Herein, to address the challenge of developing new formulations of water-in-salt electrolytes, we propose a mixed cation strategy: we use cheaper (by at least an order of magnitude) and more soluble salts featuring alkali cations beyond lithium, such as potassium, to create the water-in-salt condition. Co-dissolved lithium salts enable compatibility with traditional intercalation battery electrodes. We show that potassium acetate-based highly concentrated electrolytes can provide the same benefits of the extended voltage window as imide-based electrolytes and, once combined with lithium acetate, demonstrate compatibility with traditional Li-ion battery electrode materials while being low-cost and environmentally benign.